2022 IMEKO TC-4 International Conference on
Metrology for Archaeology and Cultural Heritage
University of Calabria, Italy, October 19-21, 2022

# Raman and micromorphological characterization of carbonates in plaster-like materials from the Natufian site of Eynan (Ain Mallaha), Israel

Leila Es Sebar[1], Leonardo Iannucci[1], Sabrina Grassini[1], Emma Angelini[1], Rivka Rabinovich[2,3], Anne Bridault[4], Hamoudi Khalaily[5], François R. Valla[6], Yuval Goren[7]

[1]*Department of Applied Science and Technology, Politecnico di Torino, Turin, Italy, leila.essebar@polito.it, leonardo.iannucci@polito.it, sabrina.grassini@polito.it, emma.angelini@polito.it*
[2]*Institute of Archaeology, The Hebrew University of Jerusalem, Jerusalem, Israel, rivkar@mail.huji.ac.il*
[3]*Institute of Earth Sciences, National Natural History Collections, The Hebrew University of Jerusalem, Jerusalem, Israel*
[4]*UMR 7041ArScAn, CNRS, MSH Mondes, Archéologies Environnementales, 21 allée de l'Université, 92000 Nanterre, France, anne.bridault@cnrs.fr*
[5]*Israel Antiquities Authority, P.O.B. 586, 91004 Jerusalem, Israel, hamudi@israntique.org.il*
[6]*C.N.R.S., ArScAn. Maison René-Ginouvès, 21 Allée de l'Université, 92000 Nanterre, France, francois.valla@wanadoo.fr*
[7]*Department of Archaeology, Ben-Gurion University of the Negev, PO Box 653, 8410501 Beer Sheva, Israel, ygoren@bgu.ac.il*

***Abstract* – The archaeological site of Eynan, located by the spring of Ain Mallaha and on the shores of Lake Hula in the Upper Jordan Valley, Israel, existed for several millennia at the end of the Pleistocene. During the Natufian culture of the Levantine Epipalaeolithic, the site was one of the largest known occupations in the Levant for some millennia (ca. 14,300 - 11,900 cal BP). Remains of Natufian architecture were found, together with evidence of early experimenting with pyrotechnology for the creation of lime plaster. Several features were identified during the excavations as assumed lime plaster installations. Samples investigated by micromorphology methods under the polarizing microscope revealed that while all were composed of calcium carbonate, and some indeed represent anthropogenic burnt lime products, others reflected the results of post-depositional or contemporaneous natural processes rather than technological products. The study of the samples at a molecular level through Raman spectroscopy enables a new methodology for the quick distinction between the features observed by micromorphology.**

## I. INTRODUCTION

Eynan/Ain Mallaha was one of the main hamlets in the Levant to be intermittently inhabited by groups of hunters-fishers-gatherers for several millennia at the end of the Pleistocene. The Eynan people settled in the vicinity of the Hula Lake and the vast adjacent wetland area, and exploited a wide array of resources and habitats, as reflected by the plant and faunal remains at the site. During the Natufian period, the site was one of the main human settlements in the Levant, intermittently inhabited between ca. 14,300-11,900 cal BP [1].

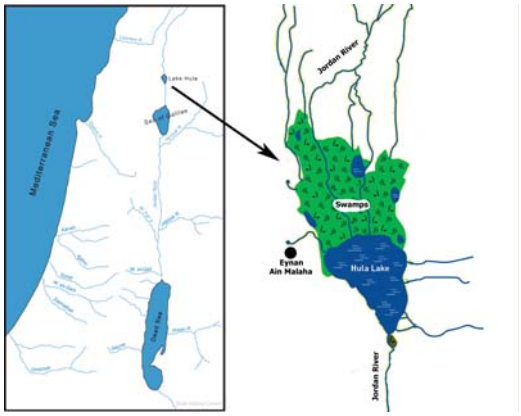


*Fig. 1. Map of the Hula Basin near the spring of Eynan-Ain Mallaha, with indications of the main natural ecological niches.*

The excavations of the Natufian settlement exposed a hamlet of semi-buried stone-built structures on a slope

overlooking the spring and south of it. The dwellings are delimited by circular or semi-circular walls, sometimes still standing more than 1 m high, which served as retaining walls. The walls are composed of a facing of raw limestone blocks applied against the vertical surface created by cutting into the slope. Installations and in one case, wall coating made of lime plaster, were observed during the excavation, being among the oldest evidence of sophisticated pyrotechnical processes in the Near East. Floors were identified thanks to these small installations, sometimes associated with partial pavements of slabs or pebbles. These indications could be combined with those provided by ash dispersals from the hearths, and by objects lying flat, to reconstruct coherent surfaces. Several buildings display more than one of these floors superimposed, sometimes linked to repairs of at least part of the wall.

During the excavations at the site, various features and facilities within the built structures, between, and around them were identified as assumed products of lime plaster. A previous study formerly conducted on lime plaster from Eynan incorporated in one of the burials was able to show through Fourier-transform infrared spectroscopy (FTIR) analyses, that it was indeed a product of pyrotechnology. This study also established a method that makes it possible to differentiate between calcium carbonate of geological origin (limestone, chalk), anthropogenic that is not a pyrotechnological product (wood ash) and pyrotechnological lime [2]. Additional studies conducted on lime plaster products from the Natufian phase to the end of the Pre-Pottery Neolithic period, established the research methods that combine the use of micromorphology and FTIR for the analytical scientific distinction between pyrotechnology plaster and other calcareous phenomena, either natural or the result of post-depositional processes from human activities [3].

Lime plasters are composed of different calcareous raw materials, such as calcite, aragonite, and/or dolomite, which could be mixed with some additives. Several factors can affect the characteristics of lime plaster, including the composition of the raw material employed, the technology that has been used, and the surrounding environmental conditions. Taking into consideration all these parameters, the investigation of the chemical and physical properties of lime plasters can help archaeologists and art or technology historians in gathering information about these past materials, their development, application, and conservation. Rapid and reliable characterization methods using portable equipment and non-invasive or minimally intrusive methods are highly desired, both in archaeological excavations and in museums and monuments where orthodox laboratory conditions are lacking.

Mineralogical and micromorphological characterization is often performed in archaeological contests taking advantage of thin-section optical mineralogy, allowing to perform petrographic studies to characterize the minerals and many other physical features that are present in the fabric of the artifact or sediment. On the other hand, other techniques are used to study archaeological materials, such as X-ray diffractometry (XRD), electron microscopy, X-Rays fluorescence spectroscopy (XRF), FTIR, and Raman Spectroscopy [4], [5], [6]. It is worth noticing that even if the potential of these methods proved to be useful, some of them may present significant limitations. For instance, they can require sample preparation, may be invasive and destructive, become time-consuming or require proper laboratories only. Considering these issues, during the last decade, the technology related to Raman spectroscopy has been expanding and portable solutions were developed, providing several advantages for field or outdoor analyses. Because the technique requires no, or minimal, sample preparation, the Raman spectrometer can be implemented as a portable, handheld device allowing for a "point and shoot" spectrum acquisition.

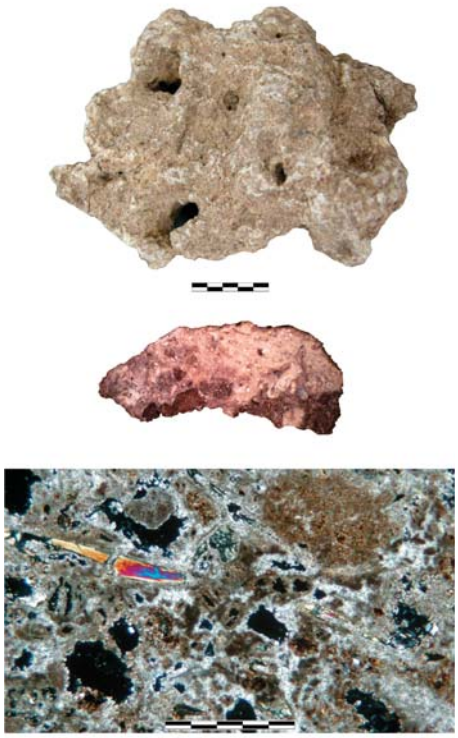

*Fig. 2. Example of one of the retrieved samples and its thin section. From the top: original sample, sample cut in half and polished, and thin section under the microscope. The scale bars for the two upper details and the photomicrograph are 1cm and 1 mm long, respectively.*

Moreover, Raman spectroscopy allows for discrimination among different molecular phases based on their vibrational states responsible for the scattering of the incident light [7]. Therefore, this study aims to combine the

mineralogical and micromorphological characterization of the lime plasters and the other calcareous "plaster-like" finds from Eynan with Raman spectroscopic techniques, in order to fully characterize these materials also at the molecular level, to provide a more complete interpretation of the various features and to equip other scholars with the ability to practice this methodology in other researches.

## II. MATERIALS AND METHODS

### A. Sampling and sample treatment

The materials investigated in this study have been retrieved from the site by the excavators (co-authors Valla and Khalaily), who considered them to be installations made of lime plaster on the basis of collected data [1]. The features were scattered in various parts of the excavated area - among the houses, close to them, and in some open areas. From these, material samples were removed during the excavation. Portions of these samples were later brought to the Laboratory for Microarchaeology at the Ben Gurion University of the Negev for micromorphological analysis. In the laboratory, the samples were cut in half and polished. Then half of the sample was dedicated for the preparation of micromorphological thin-sections, $30\ \mu\mathrm{m}$ in thickness, with the procedure used for petrographic characterizations [8], to be examined under the petrographic microscope. The other half was employed for Raman spectroscopy analysis.

Having two mirrored sides of the same sample enables us to perform a full characterization of the features of these materials, providing information from the petrographic microscopic and molecular points of view on the same areas. Figure 2 reports an example of a prepared untouched surface, the half-cut polished cross-section of the sample, and the thin section mirroring this polished section.

### B. Micromorphology and Petrography

Archaeological micromorphology links the microscopic analysis of intact, oriented sediment samples in thin sections with field observations of larger units. It allows for the study of depositional processes and sediment features using the polarized light microscopic analysis under plane-polarized (PPL) and cross-polarized light (XPL). This way, micro-artifacts, and residues can be studied in their in-situ context. It also allows recovering and examining a wide range of minute plant and faunal remains, such as siliceous phytoliths, charred plant tissues, microscopic bone splinters, coprolites, or their leftovers. Evidence for burning can be identified in both organic (plants, bones) and inorganic residues (through structural changes in minerals or microscopic slug and ash remains). Post-depositional alterations, such as bioturbation, organic decay, soil formation, mineral alteration, or translocation of sediments by alluviation or aeolian activities, can be also explored. Finally, micromorphological thin sections provide permanent archival samples for future research as they can always be re-examined [9, 8].

### C. Portable Raman Spectroscopy

The samples were analyzed at the molecular level using the commercial modular portable instrument, produced by BWTEK™. This is a portable Raman spectrometer using a high quantum efficiency CCD array detector with deeper cooling and a high dynamic range. It delivers an improved signal-to-noise ratio for up to $30\ \mathrm{min}$, making it possible to measure weak Raman signals. The instrument is provided with a monochromatic excitation laser, with a wavelength of $785\ \mathrm{nm}$. The emitted signal is collected by a BTC675N® spectrometer, in the range between $65\ \mathrm{cm}^{-1}$ and $3350\ \mathrm{cm}^{-1}$, with a resolution of $6\ \mathrm{cm}^{-1}$. The technique was performed directly on the surface of the sample, with a non-destructive approach, in order to characterize all the mineralogical phases identified with the microscopical investigation. It was possible to achieve this aim since the instrument was connected to the portable BAC151® compact Raman microscope, provided with several lenses able to focus the signal with a spot with a diameter of approximately $300\ \mu\mathrm{m}$, $90\ \mu\mathrm{m}$, $50\ \mu\mathrm{m}$, and $20\ \mu\mathrm{m}$. The measurements were performed using the following parameters: laser power of $30\ \mathrm{mW}$, integration time of $10\ \mathrm{s}$, 12 repetitions for each area.

To identify the several mineralogical phases, present in the samples, the collected spectra were processed using principal component analysis (PCA) by means of a Python script.

The data were pre-processed as reported in the following. After an initial observation of the spectra, only the region of interest reporting the relevant peaks was selected, narrowing the range between $250\ \mathrm{cm}^{-1}$ and $1200\ \mathrm{cm}^{-1}$. The baseline was removed by exploiting the asymmetric least squares smoothing. Then, a Savitzky-Golay filter was applied to the spectra working with a window length of $15\ \mathrm{cm}^{-1}$ and, successively, the data were fitted with a second-order polynomial. Finally, a standard normal variate transformation was applied, and the spectra were processed to extract the principal components [10].

## III. RESULTS AND DISCUSSION

### A. Micromorphology and Petrography

The petrographic characterization revealed that within all the samples there may be five different categories of calcium carbonate ($CaCO_3$) materials: lime plaster, "fossil hearths", "seasonal puddles", secondary calcite, and geogenic calcite, which will be described in the following sections.

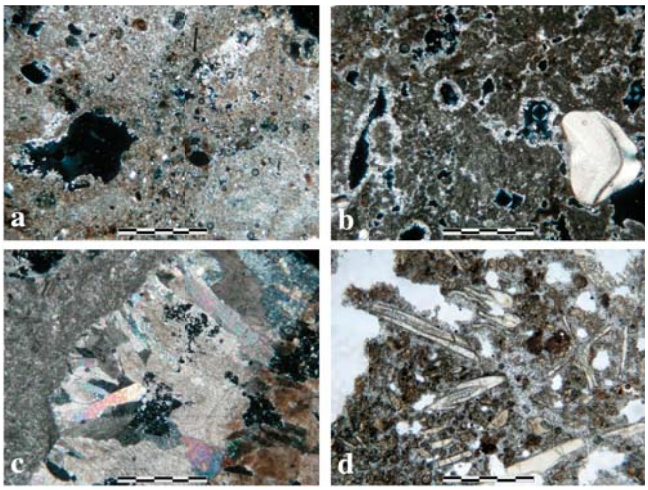


*Fig. 3. Photomicrographs of selected samples included in this study. a) Lime plaster made of fine (crypto-crystalline) calcium carbonate with limestone grain (lower right) and some secondary calcite near the void (left) (XPL); b)"fossil hearth" with ash rhombus (rhombs in the gray matrix), mollusk shell fragment (pearl-white fine crystalline body at right) and re-crystallization of secondary calcite around voids (XPL); c) geogenic calcite from a stalactite/stalagmite in the plaster matrix (XPL); d) "seasonal puddles" with dense tiny animal bones in calcitic cement/matrix (PPL). The scale bar in all photomicrographs is 1 mm long.*

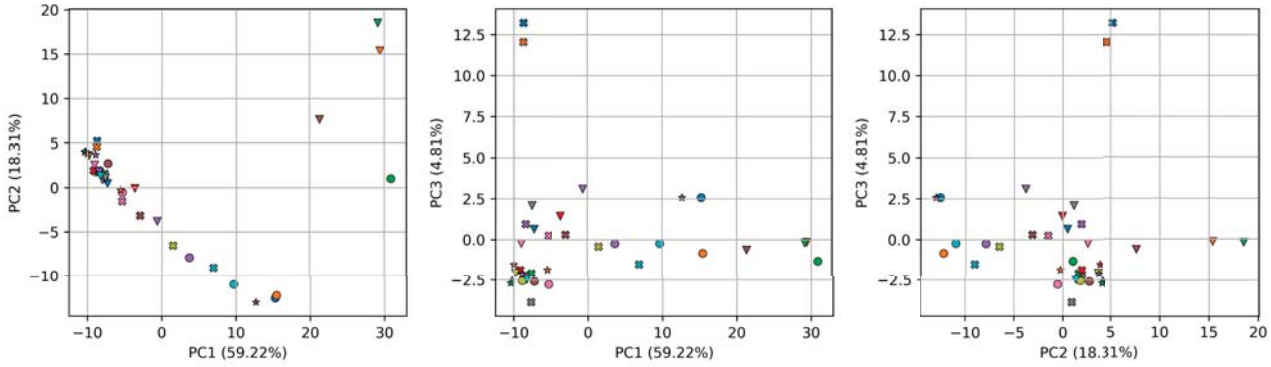


*Fig. 4. PCA Scores bi-plots of the first three components (PC1-PC2, PC1-PC3, and PC2-PC3) extracted from Raman spectroscopy data. Percent variance captured by each PC is reported in parenthesis along each axis.*

### A..1 Lime plaster

Lime plaster is calcium carbonate decalcined after heating to $750°C$ and above to create lime, then soaked in water (Eq. 1), and then, with the addition of atmospheric $CO_2$, altered back into calcium carbonate ($CaCO_3$) to form solid plaster [2].

$$\begin{aligned} CaCO_3 + heat &\rightarrow CaO + CO_2 \\ CaO + H_2O &\rightarrow Ca(OH)_2 + heat \end{aligned} \quad (1)$$

This typology of material was identified in several samples and it is produced with an anthropogenic technological process involving the intentional use of fire to change the chemical composition of materials (pyrotechnology). A representative image of a sample of lime plaster under the petrographic microscope is shown in Figure 3a: the lime plaster sample presents a fine (crypto-crystalline) calcium carbonate.

### A..2 "Fossil hearths"

Wood naturally contains calcium in the form of calcium oxalates. After burning, the resulting soft gray ash exhibits individual ash rhombs (rhombus-shaped grains), indicating that the calcareous nature of the matter is associated with ashes and burning. Hence, in micromorphology, this is an indication of ashy deposits [8]. These may be accompanied by bone fragments, shells, soil concentrations, etc., overall representing an anthropogenic activity (fireplace). Under humid conditions, such as the ones that can be found at Eynan, the carbonate may be partially precipitated in groundwater and re-crystallized to form calcitic cement, which

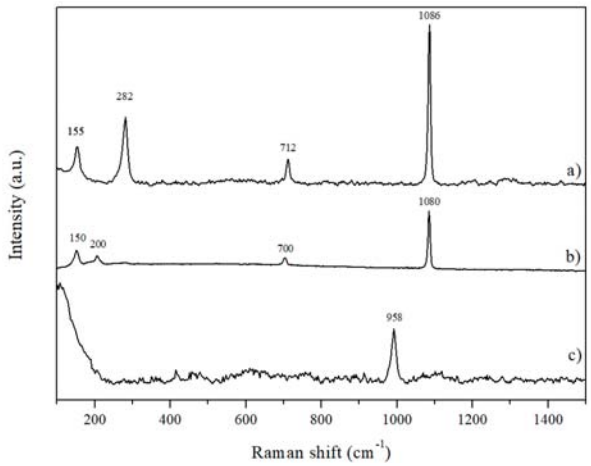


*Fig. 5. Representative Raman spectra of the main mineralogical phases identified in the characterized samples: a) calcite, b) aragonite, c) hydroxyapatite.*

holds the hearth as solid rock, often preserving the overall rounded shape, lenticular in cross-section, of the original hearth. Examples of "fossil heart" can be observed in Figure 3b.

### A..3 Geogenic calcite

Calcite of geological origin appears in the samples either as particles of limestone rocks or as fragments of calcite that accumulated naturally under terrestrial conditions, as it happens in stalactites and stalagmites. These carbonates can be distinguished under the petrographic microscope [2]. At an archaeological site, accumulations of natural chalk may also appear as a result of human activity, but these do not belong to the category of "plaster". An example of geogenic calcite is reported in Figure 3c.

### A..4 Secondary calcite

Within anthropogenic deposits of the first two categories, there may be spots where secondary crystallization of calcite took place, mainly around cavities. In these areas, calcite precipitated in water re-crystallized and grew into larger idiomorphic crystals that surround a void, representing post-depositional processes related to natural phenomena that occurred within the otherwise anthropogenic sediment [9]. Such crystal can be seen in Figure 3b, recrystallized around the voids present within the sample.

### A..5 Seasonal puddles

Two samples disclose a dense accumulation of fish or amphibian bones from millimeters to microscopic-scale dimensions, embedded in a cement matrix made of calcite mixed with some clay. There is no indication of heating in the bones or the matrix (Figure 3d). The interpretation of these features could be that of seasonal puddles that concentrated a large amount of fry in their water, and with their gradual drying, sediment was formed containing bones of the tiny fauna embedded in a calcitic cement that crystallized from the calcium dissolved in the water [9]. Such processes can certainly occur at a site located in an area of springs and on the shore of a lake because of natural seasonal processes. Therefore, the appearance of such deposits is not related to human activity but to natural environmental phenomena.

### *B. Portable Raman Spectroscopy and Principal Component Analysis (PCA)*

To discriminate among the different carbonate minerals investigated with Raman Spectroscopy, Principal Component Analysis (PCA) was employed. This kind of unsupervised multivariate analysis allows us to reduce the number of variables of the collected data, identifying the most relevant features in the spectra [10]. The data provided for the PCA consisted of the Raman spectra, after pre-processing, as described in Section C..

The results extracted from the data are reported in Figure 4 as scores biplots, in parallel for PC1-PC2, PC1-PC3, and PC2-PC3 (from left to right) components. The three components account for 59.22%, 18.31%, and 4.81% of the overall dataset variance, respectively. As it is possible to observe in the PC1/PC2 score bi-plot, the data present a clear separation in two main clusters, based on the value of the PC1 component. In particular, a group of four spectra presents PC1 values greater than 20.

In addition, in the PC1/PC3 score bi-plot, there is another evident cluster that is separated by PC3 values greater than 10. An analogous separation can be observed also in the PC2/PC3 score bi-plot.

The separation in these three main clusters can be interpreted as a result of similar composition, namely similar vibration modes. In Figure 5 a representative spectrum for each of the identified groups is displayed.

The first group, which presented PC1 values lower than 20, corresponds to the spectrum reported in Figure 5a, which is characterized by the presence of four prominent peaks, that corresponds to the most relevant features of Calcite [11]. In particular, it is possible to identify peaks at $155\ \mathrm{cm}^{-1}$, and $282\ \mathrm{cm}^{-1}$, which are related to the external vibration of the $CO_3$ group, while the $712\ \mathrm{cm}^{-1}$, and $1086\ \mathrm{cm}^{-1}$ peaks corresponds to the out-of-plane bending and stretching internal vibration modes [12]. Calcite was identified in several areas over the samples, in particular in the crystal of secondary calcite and geogenic calcite, but also in the matrix of the samples, in correspondence with both light and darker areas.

The second cluster, with PC1 values greater than 20, is associated with the spectrum reported in Figure 5c, which

was identified as hydroxyapatite based on a intense peak at $958\ \mathrm{cm}^{-1}$, related to the phosphate symmetric stretching ($\nu 1\text{-}PO_4^{3-}$) [13], [14]. This kind of spectrum is associated with the analyses carried out on the fish or amphibian bones enclosed in the calcitic matrix.

Regarding the last cluster, the major peaks assignments are $150\ \mathrm{cm}^{-1}$, $200\ \mathrm{cm}^{-1}$, $700\ \mathrm{cm}^{-1}$, and $1080\ \mathrm{cm}^{-1}$. These are the vibration modes assigned to another carbonate, namely aragonite, polymorphic modifications of calcite (Figure 5b). The strongest vibration at $1080\ \mathrm{cm}^{-1}$ corresponds to the symmetric stretching mode of the $CO_3^{2-}$ group, the one at $700\ \mathrm{cm}^{-1}$ to the asymmetric bending, while the more weak Raman bands are due to the translations and rotations of $CO_3$ groups [15], [16]. Aragonite was identified in correspondence with several shell fragments.

## IV. CONCLUSION

The research presented here focused on various phenomena representing anthropogenic, geogenic, and secondary processes that apply to sediments of anthropogenic origin after their deposition, all of which include calcium carbonate. The diagnosis of these phenomena, each of which has a different meaning for the interpretation of the archaeological record to which it is related, is important in real-time during the excavation. The study showed that after understanding the samples using the invasive method of micromorphology, they can be characterized using a Raman spectrometer and subsequently can be used in the field or at the cultural heritage site in mobile Raman to characterize similar materials by non-destructive methods. Our test case focused on the prehistoric site at Eynan, but in fact, a similar methodology can be applied to other sites and test cases as well.

## REFERENCES


[1] F. R. Valla, H. Khalaily, N. Samuelian, F. Bocquentin, A. Bridault, and R. Rabinovich, "Eynan (ain mallaha)," in *Quaternary of the Levant: Environments, Climate Change, and Humans* (Y. Enzel and O. Bar-Yosef, eds.), pp. 295–302, Cambridge University Press, 2017.

[2] V. Chu, L. Regev, S. Weiner, and E. Boaretto, "Differentiating between anthropogenic calcite in plaster, ash and natural calcite using infrared spectroscopy: implications in archaeology," *Journal of Archaeological Science*, vol. 35, no. 4, pp. 905–911, 2008.

[3] D. E. Friesem, I. Abadi, D. Shaham, and L. Grosman, "Lime plaster cover of the dead 12,000 years ago–new evidence for the origins of lime plaster technology," *Evolutionary Human Sciences*, vol. 1, 2019.

[4] G. Artioli, *Scientific methods and cultural heritage: an introduction to the application of materials science to archaeometry and conservation science*. OUP Oxford, 2010.

[5] T. de Caro, E. Angelini, and L. E. Sebar, "Application of $\mu$-raman spectroscopy to the study of the corrosion products of archaeological coins," *ACTA IMEKO*, vol. 10, no. 1, pp. 234–240, 2021.

[6] L. E. Sebar, L. Iannucci, S. Grassini, E. Angelini, M. Parvis, A. Bernardoni, A. Neuwahl, and R. Filardi, "Characterization of the santa maria del fiore cupola construction tools using x-ray fluorescence," *ACTA IMEKO*, vol. 11, no. 1, p. 7, 2022.

[7] P. Rostron, S. Gaber, and D. Gaber, "Raman spectroscopy, review," *laser*, vol. 21, p. 24, 2016.

[8] P. Goldberg and F. Berna, "Micromorphology and context," *Quaternary International*, vol. 214, no. 1-2, pp. 56–62, 2010.

[9] B. Fabbri, S. Gualtieri, and S. Shoval, "The presence of calcite in archeological ceramics," *Journal of the European Ceramic Society*, vol. 34, no. 7, pp. 1899–1911, 2014.

[10] J. Miller and J. C. Miller, *Statistics and chemometrics for analytical chemistry*. Pearson education, 2018.

[11] D. Krishnamurti, "The raman spectrum of calcite and its interpretation," in *Proceedings of the Indian Academy of Sciences-Section A*, vol. 46 (3), pp. 183–202, Springer, 1957.

[12] Y. Kim, M.-C. Caumon, O. Barres, A. Sall, and J. Cauzid, "Identification and composition of carbonate minerals of the calcite structure by raman and infrared spectroscopies using portable devices," *Spectrochimica Acta Part A: Molecular and Biomolecular Spectroscopy*, vol. 261, p. 119980, 2021.

[13] J. A. Stammeier, B. Purgstaller, D. Hippler, V. Mavromatis, and M. Dietzel, "In-situ raman spectroscopy of amorphous calcium phosphate to crystalline hydroxyapatite transformation," *MethodsX*, vol. 5, pp. 1241–1250, 2018.

[14] D. B. Thomas, C. M. McGoverin, R. E. Fordyce, R. D. Frew, and K. C. Gordon, "Raman spectroscopy of fossil bioapatite-a proxy for diagenetic alteration of the oxygen isotope composition," *Palaeogeography, Palaeoclimatology, Palaeoecology*, vol. 310, no. 1-2, pp. 62–70, 2011.

[15] Z. Tomić, P. Makreski, and B. Gajić, "Identification and spectra-structure determination of soil minerals: Raman study supported by ir spectroscopy and x-ray powder diffraction," *Journal of Raman Spectroscopy*, vol. 41, no. 5, pp. 582–586, 2010.

[16] R. G. Arroyo-Loranca, N. Y. Hernandez-Saavedra, L. Hernandez-Adame, and C. Rivera-Perez, "Ps19, a novel chitin binding protein from pteria sterna capable to mineralize aragonite plates in vitro," *PLoS ONE*, vol. 15, no. 3, 2020.